Electronic Supplementary Information for

Waterproof and breathable membranes of waterborne fluorinated polyurethane modified electrospun polyacrylonitrile fibers

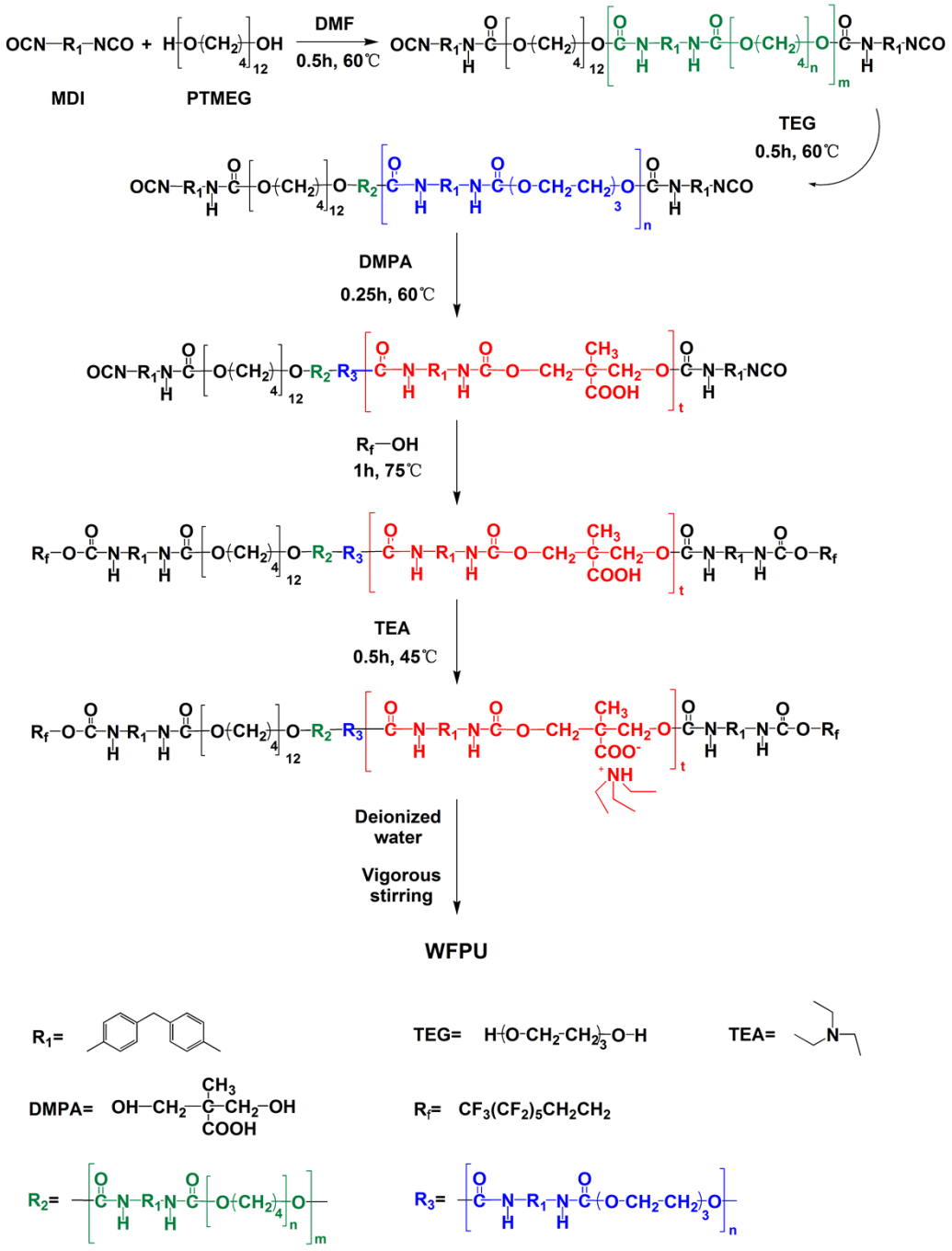

Fig. S1 Schematic diagram illustrating the strategy for preparation of WFPU emulsion.

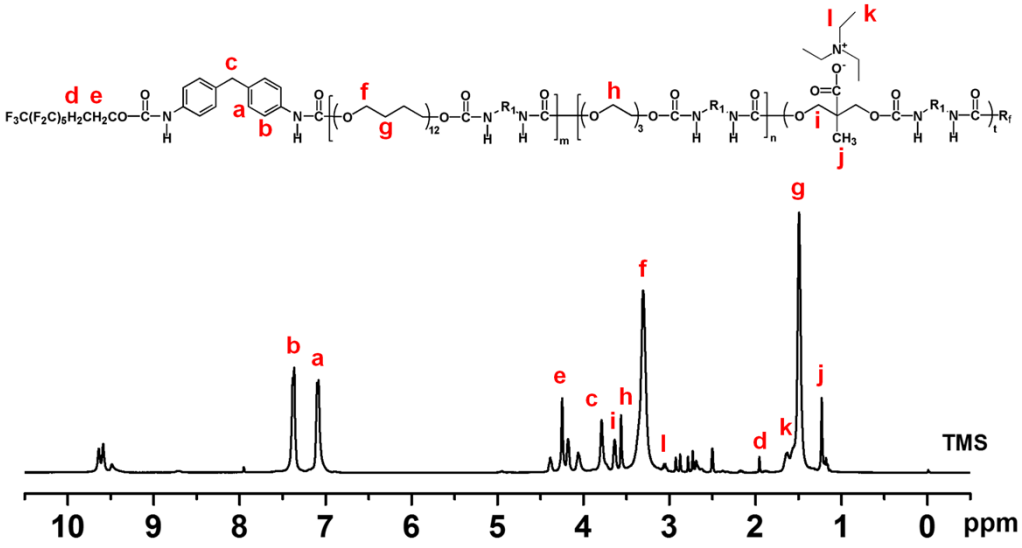

Fig S2 ^{1}H NMR spectrum of WFPU.

The WFPU after purification and crystallization was subjected to NMR spectroscopic analysis. Fig. S2 present the chemical structure and ^{1}H NMR spectrum of WFPU. The signals for aromatic protons of MDI groups appeared between 7.08 to 7.35 ppm and for -CH_2- appeared at 3.81 ppm (Fig. S2a-c). The chemical shift for -CH_2-CH_2- in terminal fluorinate segments appeared at 1.89 and 4.08 ppm (Fig. S2d and e). For PTMEG segments, the shifts for -O-CH_2- and -CH_2-CH_2- appeared at 3.37 and 1.46 ppm, respectively, as shown in Fig. S2f and g. For TEG segments, the protons of–O-CH_2-CH_2-O- given their signals at 3.56 ppm (Fig. S2h). For DMPA groups, the protons of -O-CH_2- given their signal at 3.78 ppm (Fig. S2i), and the chemical shifts for -CH_3 group appeared at 1.27 ppm (Fig.S2j). The protons of -CH_2- and -CH_3 groups in TEA given their signal at 1.56 and 3.28 ppm, respectively, as shown in Fig. S2k and l.

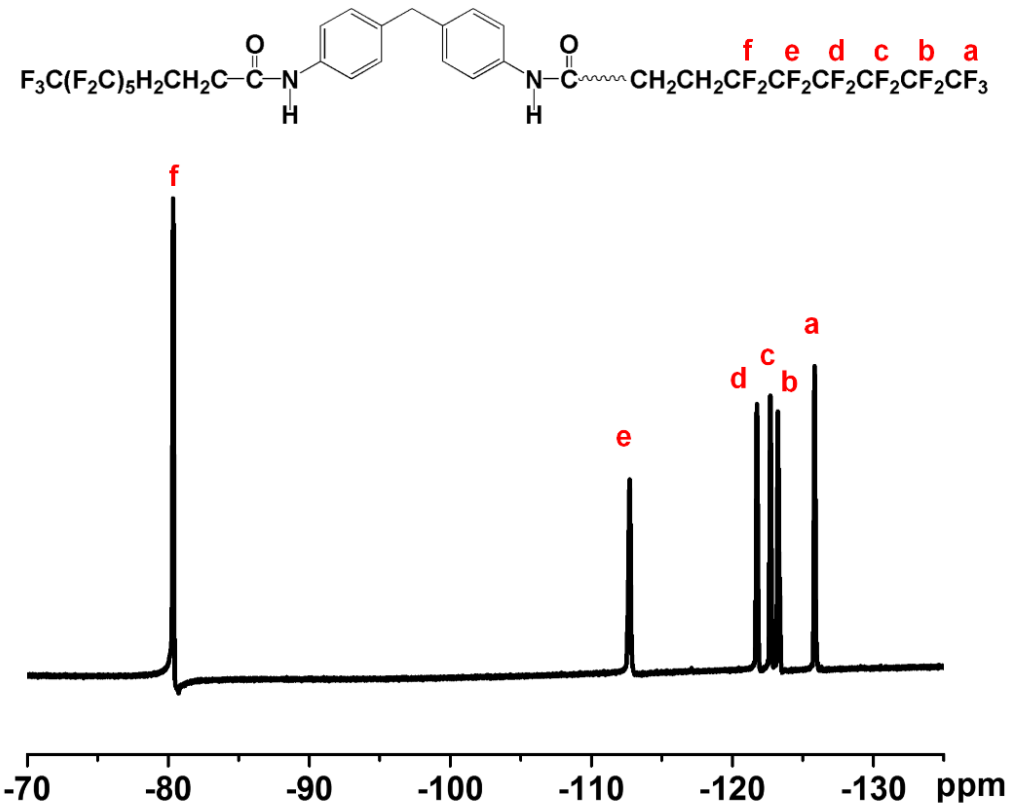

Fig. S3 ^{19}F NMR spectrum of WFPU.

^{19}F NMR has given further structural affirmation of FPU (Fig. S3). The chemical shift for terminal CF_3 appeared at 80.36 ppm, while for $-CF_2-CH_2-$ appeared at 125.83 ppm. The remaining $-CF_2-$ has given their chemical shift between 112.71 to 123.22 ppm. Acquisition of quantitative results from NMR analysis has confirmed the chemical structure of WFPU.

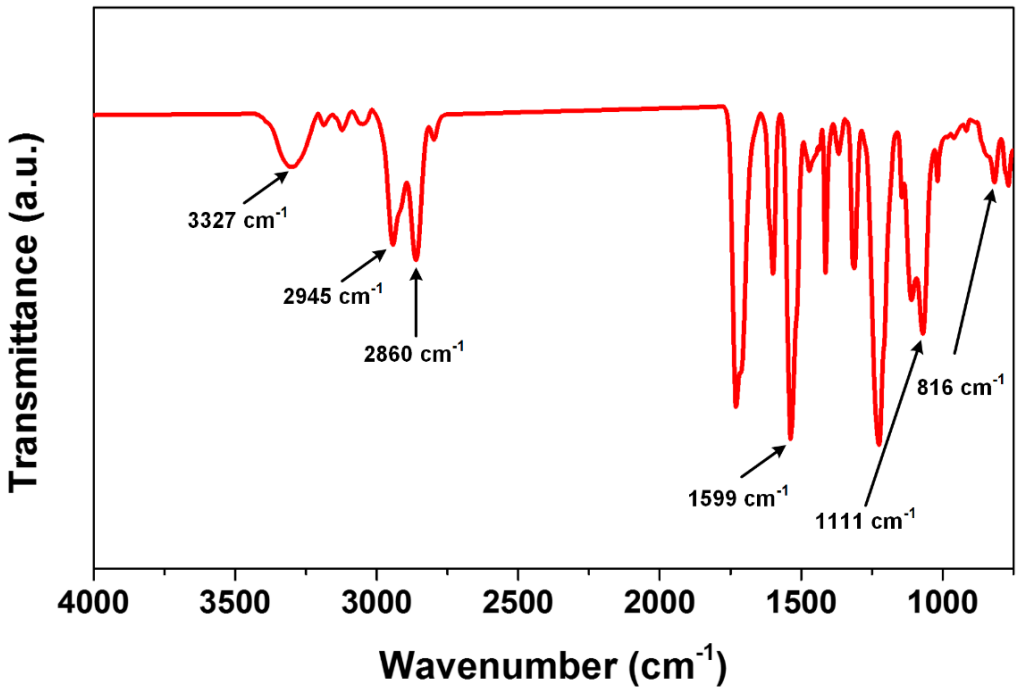

Fig. S4 FT-IR spectrum of WFPU.

Fig. S4 shows the FT-IR spectrum of WFPU. The typical absorption features for carbamate group were found at 3326 cm^{-1} (N-H), 1710 cm^{-1} (C=O), 1538 cm^{-1} (N-H) and 1111 cm^{-1} (C-O-C), respectively. The $-CH_2-$ specific for PTMEG has given their absorption band at 2945 and 2860 cm^{-1}. The stretching vibration for aromatic ring of MDI was found at 1600 cm^{-1}. The stretching vibration from $-CF_3$ and deformation vibration for CF_2 were found at 1225 and 816 cm^{-1}, respectively.

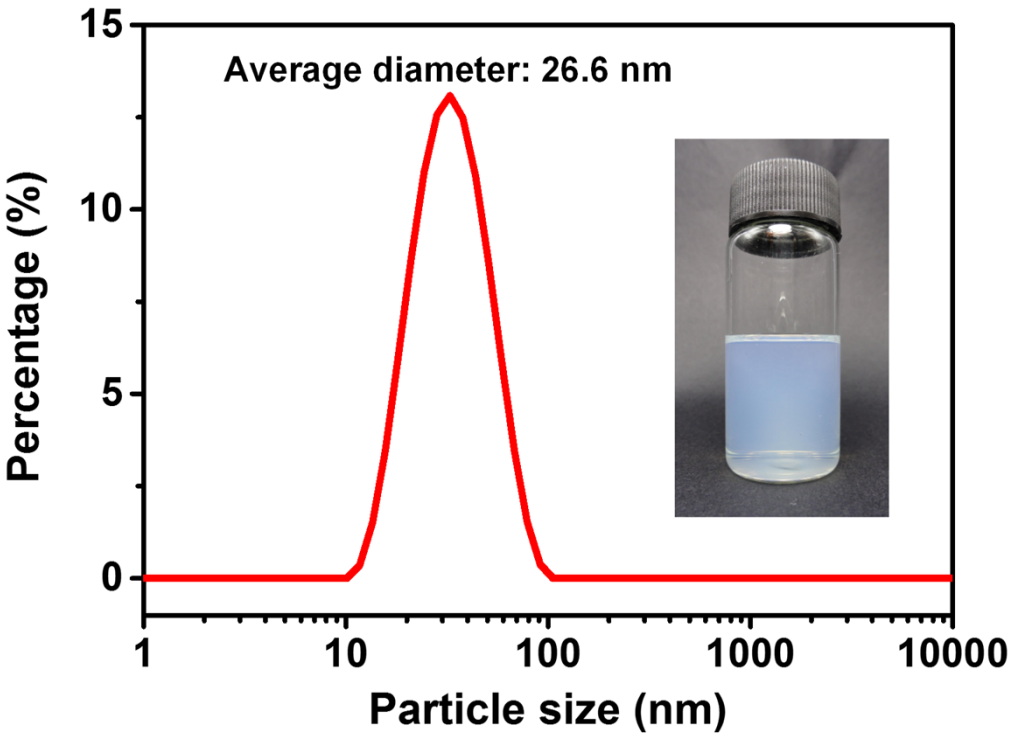

Fig. S5 The particle size distribution of WFPU emulsion.

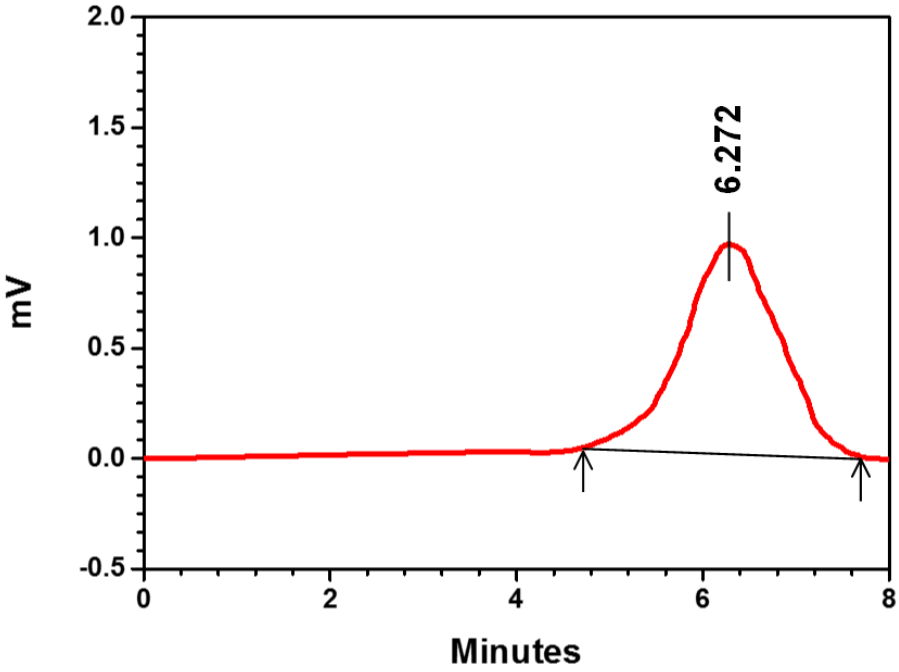

M_n (g/mol)	M_w (g/mol)	M_z (g/mol)	M_{z+1} (g/mol)	Polydispersity
21759	31120	43184	55433	1.43

Fig. S6 GPC curve of the as-synthesized WFPU and the molecular weight and distribution results.

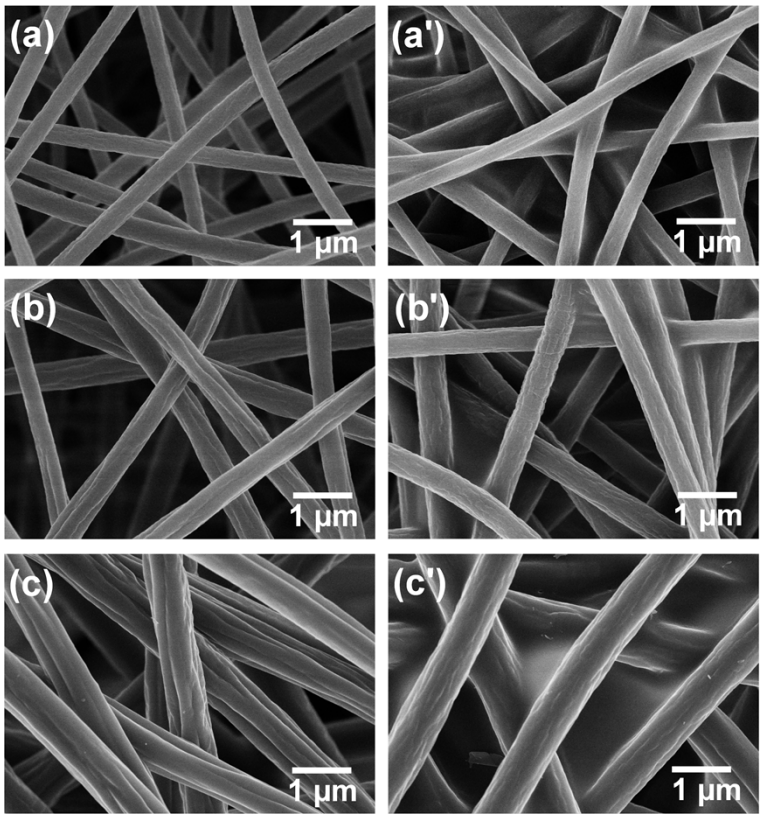

Fig. S7 FE-SEM images of (a) PAN-10, (a') WFPU-5@PAN-10, (b) PAN-12, (b') WFPU-5@PAN-12, (c) PAN-14, and (c') WFPU-5@PAN-14 fibrous membranes.

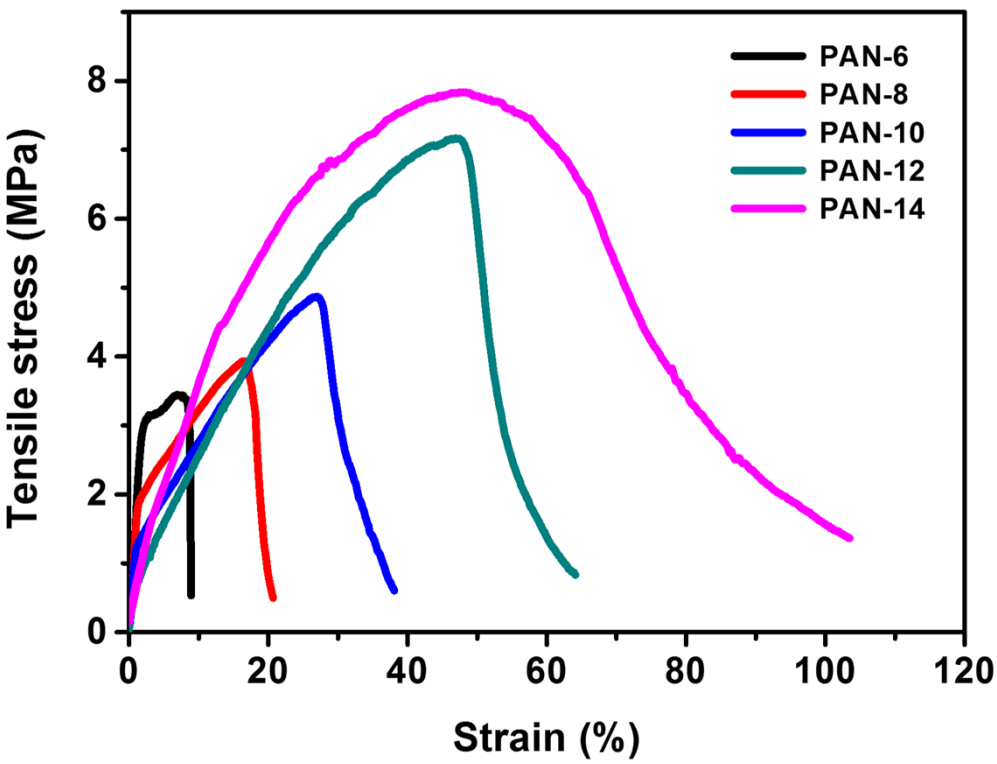

Fig. S8 Stress-strain curves of PAN fibrous membranes.

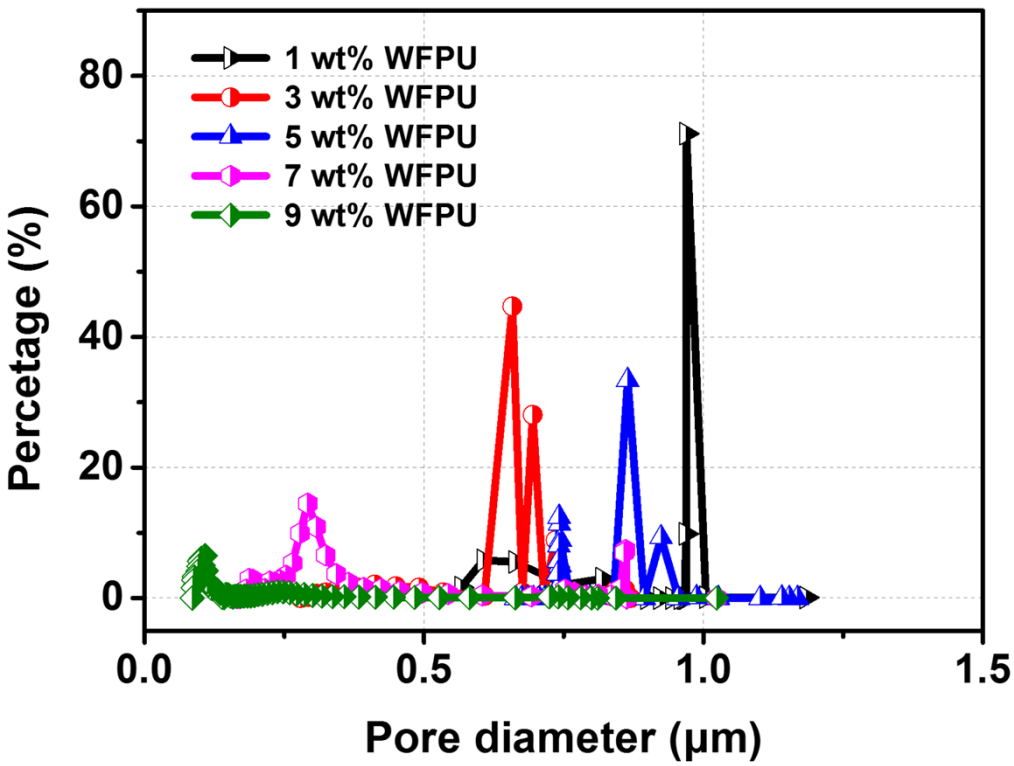

Fig. S9 Pore diameter distribution of WFPU@PAN fibrous membranes modified with WFPU emulsions of various concentrations.

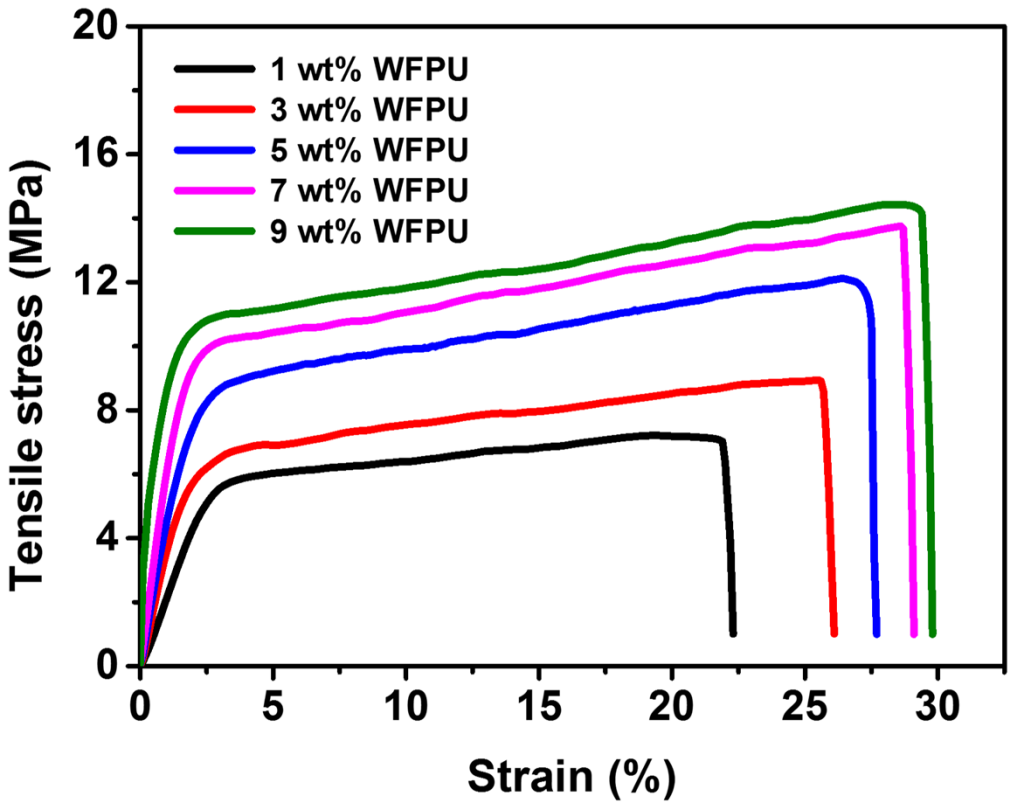

Fig. S10 Stress-strain curves of WFPU@PAN-8 fibrous membranes.

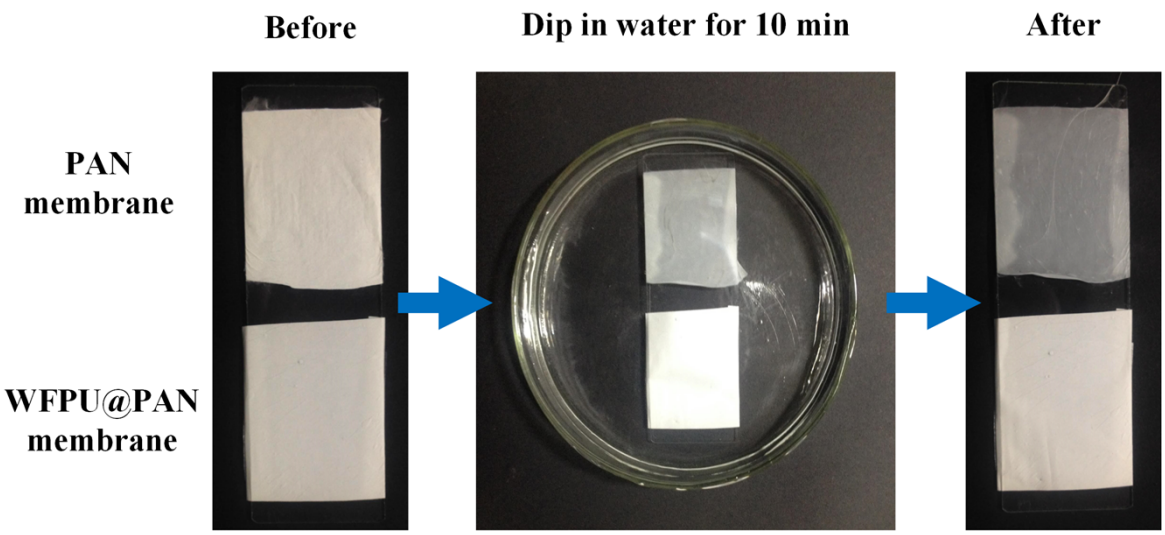

Fig. S11 Optical images of the PAN and WFPU@PAN membranes before and after dipping in water.

The PAN and WFPU@PAN membranes were fixed on a slide glass and dipped in water for 10 min. The PAN membrane was completely soaked and became translucent. However, the surface of the WFPU@PAN membrane was still dry, and not even a drop of water remained. The comparison strongly supported that the PAN fibers were completely covered by the WFPU polymer.

Table S1 d_{max} of WFPU@PAN-8 fibrous membranes modified with WFPU emulsions of various concentrations.

Specimen	d_{max} **(μm)**
WFPU-1@PAN-8	1.3
WFPU-3@PAN-8	1.2
WFPU-5@PAN-8	1.3
WFPU-7@PAN-8	1.2
WFPU-9@PAN-8	1.2